Loughborough University

This item was submitted to Loughborough's Research Repository by the author.
Items in Figshare are protected by copyright, with all rights reserved, unless otherwise indicated.

The direct synthesis of sulfobetaine-containing amphiphilic block copolymers and their self-assembly behavior

PLEASE CITE THE PUBLISHED VERSION

http://dx.doi.org/10.1016/j.eurpolymj.2016.09.002

PUBLISHER

Elsevier

VERSION

VoR (Version of Record)

PUBLISHER STATEMENT

This work is made available according to the conditions of the Creative Commons Attribution 4.0 International (CC BY 4.0) licence. Full details of this licence are available at: http://creativecommons.org/licenses/ by/4.0/

LICENCE

CC BY-NC-ND 4.0

REPOSITORY RECORD

Doncom, Kay E.B., Helen Willcock, and Rachel K. O'Reilly. 2017. “The Direct Synthesis of Sulfobetaine-containing Amphiphilic Block Copolymers and Their Self-assembly Behavior”. figshare. https://hdl.handle.net/2134/24023.

European Polymer Journal 87 (2017) 497–507

Contents lists available at ScienceDirect

European Polymer Journal

journal homepage: www.elsevier.com/locate/europolj

The direct synthesis of sulfobetaine-containing amphiphilic block copolymers and their self-assembly behavior

Kay E.B. Doncom [a], Helen Willcock [b], Rachel K. O'Reilly [a,*]

[a] Department of Chemistry, University of Warwick, Gibbet Hill, Coventry CV4 7AL, United Kingdom
[b] Department of Materials, Loughborough University, Epinal Way, LE11 3TU, United Kingdom

ARTICLE INFO

Article history:
Received 18 July 2016
Received in revised form 31 August 2016
Accepted 1 September 2016
Available online 4 September 2016

Keywords:
Sulfobetaines
Thermo-responsive polymers
Self-assembly
Controlled release
Static light scattering

ABSTRACT

Diblock copolymers containing the thermo-responsive sulfobetaine, [2-(methacryloyloxy) ethyl] dimethyl-(3-sulfopropyl) ammonium hydroxide (DMAPS), were synthesized by the aqueous RAFT polymerization of DMAPS, followed by direct chain extension in hexafluoroisopropanol (HFIP) with methyl methacrylate (MMA). This was shown to give lower dispersity polymers than RAFT emulsion polymerization. The diblock copolymers self-assembled in water to form micelles, as analyzed by light scattering (LS) and transmission electron microscopy (TEM). Micelles formed from diblocks bearing a long PDMAPS block were shown to swell with temperature, rather than display a traditional UCST cloud point. This was due to the polymers retaining hydrophilicity, even at temperatures well below the UCST for the corresponding PDMAPS homopolymer, as shown by variable temperature NMR. This swelling behavior was utilized in the release of a hydrophobic dye in response to temperature. This approach has great potential for applications in controlled release whilst maintaining the structure of the carrier nanoparticles.
© 2016 The Authors. Published by Elsevier Ltd. This is an open access article under the CC BY license (http://creativecommons.org/licenses/by/4.0/).

1. Introduction

Polymeric betaines are a class of zwitterionic polymers in which the cationic and anionic functional groups are located on the same monomer unit [1]. This unique functionality allows the polymer to undergo different types of self-association, from intramonomer, to intrachain and interchain aggregation, leading to salt-responsive and thermo-responsive behavior [2]. These polymers are often insoluble in pure water, at room temperature, but increase in solubility with the addition of salt [1,3–6]. Betaines can be further subdivided into three classes; sulfobetaines [6], phosphobetaines [7], and carboxybetaines [8], which differ in the chemical nature of the ionic groups. Sulfo- and phosphobetaines have been shown to be biocompatible, [9–14] to reduce bacterial adhesion and protein fouling [10,15] and are potentially finding uses in gene delivery,[16] blood-inert surfaces [17], and wound care [18]. Some sulfobetaines also display an upper critical solution temperature (UCST) thermo-responsive behavior, with the overall molecular weight of the polymer affecting the UCST cloud point [19–22]. An additional benefit of sulfobetaines is that the zwitterionic functionality is essentially independent of pH.

There are several reports of sulfobetaine monomers being polymerized by RAFT polymerization techniques, both as homopolymers and as block copolymers [3,21–28]. An advantage of this direct polymerization of the sulfobetaine monomer is that it can be carried out in water or salt solutions, thereby avoiding the need for organic solvents. The ability to synthesize betaine-containing diblock copolymers leads to interesting self-assembly and thermo-responsive behavior. Donovan et al.,

* Corresponding author.
E-mail address: rachel.oreilly@warwick.ac.uk (R.K. O'Reilly).

http://dx.doi.org/10.1016/j.eurpolymj.2016.09.002
0014-3057/© 2016 The Authors. Published by Elsevier Ltd.
This is an open access article under the CC BY license (http://creativecommons.org/licenses/by/4.0/).

utilized RAFT polymerization to synthesize several diblocks consisting of an N-methylacryamide sulfobetaine and dimethylacrylamide. These were found to self-assemble into micelles in pure water but formed unimers upon dissolution into 0.5 M NaCl solution [23]. We recently reported the thermo-responsive disassembly of di- and triblock copolymers consisting of sulfobetaine monomer and poly(oligioethylene glycol) methyl ether methacrylate (POEGMA) and found that the temperature at which disassembly occurs was a result of the overall hydrophilicity of the polymer, provided by the hydrophilic POEGMA blocks [29]. Arotçaréna et al. synthesized a schizophrenic block copolymer consisting of DMAPS and N-isopropylacrylamide, NIPAM, by Atom Transfer Radical Polymerization (ATRP). Self-assembly at temperatures below the UCST of the sulfobetaine block resulted in micelles with a sulfobetaine core and a hydrated PNIPAM corona, whilst at temperatures above the LCST of the NIPAM block, inverse micelles with the NIPAM block as the core and the sulfobetaine block as the hydrophilic corona were formed [9]. A similar example utilizes a diblock of a methacrylamido sulfobetaine and NIPAM synthesized by RAFT polymerization [21].

These previous examples all demonstrate amphiphilic copolymers where the non-betaine block is, under the correct conditions, hydrophilic. There are fewer examples where a permanently hydrophobic block is utilized. One reason for this is the difficulty in selecting a solvent in which both the betaine block and the hydrophobic block are soluble.

One way to address this problem is to utilize a post-polymerization betainization method, whereby the corresponding tertiary amino-monomer is polymerized in a suitable solvent and then the sulfonate group is introduced by reaction with 1,3 propane sultone or larger ring derivatives [25–27,30,31]. Copolymerization of the tertiary amine monomer with the desired hydrophobic monomer would then give access to sulfobetaine-containing polymers with hydrophobic fractions [25–27,32–34]. However, a disadvantage of this route is the toxicity of the sultones required for modification and often for more hindered tertiary amines, the reaction takes several days and does not go to completion [27,30,35]. Woodfield et al. utilized a slightly different method, whereby they synthesized a homopolymer of pentafluorophenyl acrylate and then modified by post-polymerization methods using a mixture of zwittierionic amine and hydrophobic amines, such as benzyl amine and pentyl amine. The UCST of the resulting polymer increased as the incorporation of benzyl amine, and therefore the overall hydrophobicity of the polymer, increased. However, an increase in the corporation of pentyl amine did not result in a changing UCST, which was attributed to entropic contribution from the flexible pentyl chains [36].

The direct copolymerization of hydrophobic and sulfobetaine monomers is a tougher synthetic challenge, owing to the poor solubility of the sulfobetaine block. Free radical copolymerization of sulfobetaine and hydrophobic monomers has been attempted in various solvents, including in DMSO [37,38], ethanol [39], trifluoroethanol [40]. acetonitrile/water mixtures [41] and in water as an emulsion polymerization [42,43]. However, for these solvents solubility of the growing polymer chain is problematic and can only be achieved at low sulfobetaine loadings. Free radical copolymerization of a sulfobetaine monomer and ethyl acrylate in ethanol resulted in the resulting polymer being insoluble at zwitterionic loadings higher than 10 mol% [44]. Ionic liquids have also been investigated as a better solvent for this type of copolymerization [41,45], and whilst a sulfobetaine homopolymer became insoluble during the polymerization, copolymers of *n*-butyl acrylate and sulfobetaine monomer formed a transparent gel. However purification proved problematic, as separation of the ionic liquid from the zwitterionic polymer was difficult [41].

Herein we report the direct synthesis of sulfobetaine-containing amphiphilic diblock copolymers, in a suitable solvent for both the sulfobetaine macroCTA and the growing hydrophobic chain, by RAFT polymerization and report on their self-assembly and thermo-responsive behavior. This is of interest because it allows easy access to well-defined amphiphilic betaine-containing polymers, and therefore higher order polymer structures, without the need for arduous post-polymerization modification steps.

2. Experimental

2.1. Materials

[2-(Methacryloyloxy)ethyl]dimethyl-(3-sulfopropyl)ammonium hydroxide (DMAPS), methyl methacrylate (MMA), 4-cyano-4-(phenylcarbonothioylthio)pentanoic acid (CPTA) and 4,4′-azobis(4-cyanopentanoic acid) (ACVA) were used as received from Aldrich and Fluka unless otherwise stated. AIBN [2,2′-azobis(2-methylpropionitrile)] was recrystallized twice from methanol and stored in the dark at 4 °C. Hexafluoroisopropanol (HFIP) was obtained from Fluorochem and Apollo.

2.2. Characterization

^{1}H Nuclear magnetic resonance (NMR) experiments were performed on a Bruker 400 FT-NMR spectrometer operating at 400 MHz using deuterated solvents. Chemical shifts are reported in parts per million relative to H_2O (4.79 ppm) or HFIP (4.4 ppm). Spectra were recorded at either 25 °C or 45 °C. Size exclusion chromatography (SEC) measurements were obtained in either HPLC grade HFIP at a flow rate of 1 mL min^{-1}, on a set of two HFIPgel columns plus a guard column or in pH 8.2 phosphate buffer at a flow rate of 1 mL min^{-1}, on a set of one PL aquagel OH 50 and one PL aquagel mixed M plus a PL aquagel OH guard column. Cirrus SEC software was used to analyze the data using poly(methylmethacrylate) (PMMA) or poly(ethylene glycol) (PEG) standards.

dn/*dc* measurements were recorded on a Shodex RI-101 differential refractometer. 4 concentrations between 0.5 and 2 mg mL^{-1} were run. SLS and DLS measurements were recorded simultaneously on an ALV CGS3 spectrometer consisting of a 22 mW HeNe laser at λ = 632.8 nm. Measurements were carried out at 20 °C and recorded at 7 scattering angles between 20 and 150°. The scattering vector was defined as;

$$q = \frac{4\pi\eta}{\lambda\left[\sin\frac{\theta}{2}\right]}$$

where η is the refractive index of the solvent. Concentrations between 0.1 and 2 mg mL^{-1} were analyzed for each sample. At least two measurements were run on each angle, each run for at least 100 s to determine the auto correlation function, $g_2(t)$, from DLS and the mean scattered intensity, *I*, from SLS. The resulting correlation functions were analyzed using REPES programme [46]. The R_h for the fast mode was determined by plotting the apparent diffusion coefficient for each concentration, D_{fast}, against concentration and extrapolating to zero concentration. $Kc/R_{\theta,fast}$ *vs* q^2 was plotted and from this the molecular weight and R_g for the nanostructure were determined.

Transmission electron microscopy (TEM) characterization was carried out using lacey carbon grids that had been treated with graphene oxide (GO).[47] GO solutions were synthesized as previously described [48]. One drop of GO solution was deposited onto an argon plasma treated lacey carbon copper grid and left to air dry. 4 μL of 0.1 mg mL solution of **4** was deposited onto the grid and blotted off after 30 s. Dry state TEM analysis was performed on a JEOL 2000FX microscope operating at 200 keV.

As a consequence of particle aggregation and film formation in dry state TEM, TEM samples were also prepared by the freeze-drying method [49]. 5 μL of a 0.1 mg mL^{-1} self-assembled solution of **3** was frozen onto a lacey carbon grid and the water then removed by lyophilization. This method is not ideal due to the damage that can occur to the grid upon freezing. It was obvious to see the micelles on the grid bars, as there was little graphene oxide left on the grid after freezing.

2.3. Synthesis of DMAPS homopolymers, *1* and *2*

Two DMAPS homopolymers of differing molecular weight, **1** and **2**, were synthesized by RAFT polymerization, the general procedure for which is detailed below. In order to achieve the different block lengths for **1** and **2**, varying ratios of DMAPS to CPTA were used. CPTA (10 mg, 0.004 mmol, 1 equiv.), DMAPS (5 g, 17.9 mmol. 500 equiv.) and ACVA (2 mg, 0.001 mmol, 0.2 equiv.) were dissolved in 25 mL 0.5 M NaCl solution. The pH of the solution was adjusted to ca. pH 7 (to ensure solubility of the CTA) and then degassed by bubbling with nitrogen for 40 min. The polymerization mixture was then heated to 65 °C for 19 h. The conversion was calculated from the integration of the monomer signals at δ = 5.7 and 6.1 ppm to the polymer peaks at δ = 2.2, 2.9, 3.6 and 3.8 ppm. The polymer was purified by dialysis (MWCO 3.5 kDa) and recovered by lyophilization to yield a pink polymer, **1**, M_n (^{1}H NMR) = 111.6 kDa, M_n (SEC) = 59.7 kDa, $Đ_M$ = 1.09. The DP of 400 was determined by conversion ^{1}H NMR spectroscopy. In this longer polymer the CTA end groups were not visible by ^{1}H NMR spectroscopy due to the higher molecular weight of the polymer.

^{1}H NMR spectroscopy (400 MHz, 0.5 M NaCl in D_2O): δ = 0.8–2.4 (m, 2800H, $CH_2C(CH_3)$ of polymer backbone, $CH_2C(CH_3)$ of polymer backbone, $CH_2CH_2SO_3^-$ of DMAPS side chain), 3.05–3.14 (br s, 800H, $CH_2CH_2SO_3^-$ of DMAPS side chain), 3.20–3.30 (br s, 2400H, $N^+(CH_3)_2$ of DMAPS side chain), 3.60–4.10 (m, 1600H, $N^+(CH_3)_2CH_2$ of DMAPS side chain, OCH_2CH_2N of DMAPS side chain), 4.40–4.70 (br s, 800H, OCH_2CH_2N of DMAPS side chain). ^{13}C NMR spectroscopy (125 MHz, 0.5 M NaCl in D_2O): δ = 18.5, 44.9, 45.1, 47.5, 51.6, 59.2, 62.2, 63.4, 177.4, 177.9.

Homopolymer **2**, M_n (^{1}H NMR) = 35.2 kDa, M_n (SEC) = 32.3 kDa, $Đ_M$ = 1.11. The degree of polymerization of the DMAPS block was determined to be 125 from integration of the end group signals between δ 7.50–8.10 ppm relative to the polymer peaks at 3.0 ppm and 3.34 ppm (see ESI). This matched well with that predicted from conversion ^{1}H NMR spectroscopy.

^{1}H NMR spectroscopy (400 MHz, 0.5 M NaCl in D_2O): δ = 0.8–2.4 (m, 884H, $CH_2C(CH_3)$ of polymer backbone, $CH_2C(CH_3)$ of polymer backbone, $CH_2CH_2SO_3^-$ of DMAPS side chain), 3.05–3.14 (br s, 250H, $CH_2CH_2SO_3^-$ of DMAPS side chain), 3.20–3.30 (br s, 750H, $N^+(CH_3)_2$ of DMAPS side chain), 3.60–4.10 (m, 500H, $N^+(CH_3)_2CH_2$ of DMAPS side chain, OCH_2CH_2N of DMAPS side chain), 4.40–4.70 (br s, 250H, OCH_2CH_2N of DMAPS side chain), 7.50–8.10 (m, 5H Ar*H* of CTA). ^{13}C NMR spectroscopy (125 MHz, 0.5 M NaCl in D_2O): δ = 18.5, 18.9, 19.6, 45.1, 47.5, 51.6, 59.2, 62.4, 63.4, 177.5, 178.1, 222.9.

2.4. Synthesis of PDMAPS-b-PMMA diblock copolymers

2.4.1. Synthesis of *3* in HFIP

1 (0.5 g, 0.005 mmol, 1 equiv.), MMA (0.1 g, 0.05 mmol, 200 equiv.) and AIBN (0.15 mg, 0.0005 mmol, 0.1 equiv.) were dissolved in HFIP with a small amount of DMF as an internal ^{1}H NMR spectroscopy standard. The solution was bubbled with nitrogen for 40 min and placed in a preheated oil bath at 65 °C. The polymer was purified by precipitation into methanol followed by dialysis (MWCO 12–14 kDa) and recovered by lyophilization to yield **3**, M_n (^{1}H NMR) = 121.7 kDa, M_n (HFIP SEC) = 73.1, $Đ_M$ = 1.34. ^{1}H NMR spectroscopy (400 MHz, HFIP): δ = 0.8–2.7 (m, 3360H, $CH_2C(CH_3)$ of polymer backbone, $CH_2C(CH_3)$ of polymer backbone, $CH_2CH_2SO_3^-$ of DMAPS side chain), 3.0–3.40 (m, 3200H, $CH_2CH_2SO_3^-$ of DMAPS side chain and $N^+(CH_3)_2CH_2$ of DMAPS side chain), 3.6–4.0 (br s, 1936H, $N^+(CH_3)_2CH_2$ of DMAPS side chain, OCH_2CH_2N of DMAPS side chain, OCH_3 of MMA side chain), 4.4–4.8 (br s, 800H, OCH_2CH_2N of DMAPS side chain).

*2.4.2. Synthesis of **4** via emulsion polymerization*

2 (0.1 g, 0.003 mmol, 1 equiv.) and ACVA (1 mg, 0.0004 mmol, 0.1 equiv.) were dissolved in 10 mL 0.5 M NaCl solution. The solution was then purged with nitrogen for 1 h. MMA was bubbled with nitrogen separately for ten minutes and then 104 μL (0.1 g, 1 mmol, 350 equiv.) was transferred to the polymer solution. The reaction was stirred vigorously and placed in a pre-heated oil bath at 65 °C for 16 h, by which point the solution had turned opalescent. The polymer was purified by dialysis and recovered by lyophilization to yield **4**, M_n (^{1}H NMR) = 52.2 kDa, M_n (HFIP SEC) = 31.6 kDa, $Đ_M$ = 1.80. ^{1}H NMR spectroscopy (400 MHz, HFIP): δ = 0.8–2.7 (m, 845H, $CH_2C(CH_3)$ of polymer backbone, $CH_2C(CH_3)$ of polymer backbone, $CH_2CH_2SO_3^-$ of DMAPS side chain), 3.0–3.40 (m, 1000H, $CH_2CH_2SO_3^-$ of DMAPS side chain and $N^+(CH_3)_2CH_2$ of DMAPS side chain), 3.6–4.0 (br s, 1050H, $N^+(CH_3)_2CH_2$ of DMAPS side chain, OCH_2CH_2N of DMAPS side chain, OCH_3 of MMA side chain), 4.4–4.8 (br s, 250H, OCH_2CH_2N of DMAPS side chain). ^{13}C NMR spectroscopy (125 MHz, HFIP): δ = 15.2, 17.2, 44.3, 44.7, 51.4, 179.5, 180.1, 180.5.

3. Results and discussion

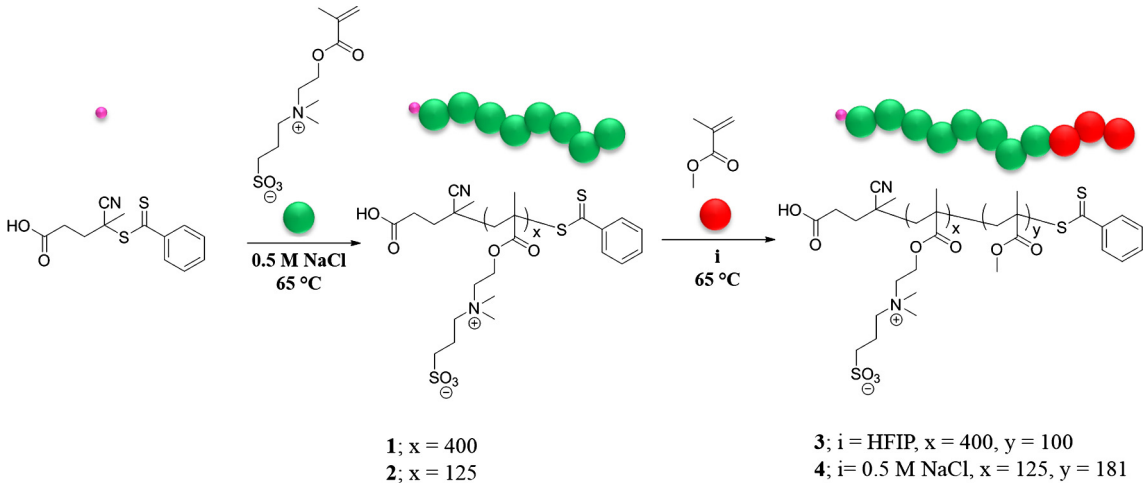
*3.1. Synthesis of PDMAPS homopolymers, **1** and **2***

Two homopolymers of PDMAPS varying in chain length (**1** and **2**) were synthesized by aqueous RAFT polymerization in 0.5 M NaCl solution, adjusted to pH 7. The salt solution was used to ensure the solubility of both the monomer and the growing polymer chain throughout the polymerization whilst adjusting the pH of the polymerization using diluted NaOH ensured both the CTA and the initiator were fully solubilized. After heating to 65 °C for 19 h the resulting polymers were purified by exhaustive dialysis against water and recovered by lyophilization to yield **1**, M_n (^{1}H NMR) = 111.6 kDa, M_n (Aq. SEC) = 59.7 kDa, $Đ_M$ = 1.09 and **2**, M_n (^{1}H NMR) = 35.2 kDa, M_n (Aq. SEC) = 32.3 kDa, $Đ_M$ = 1.11 (see ESI). Due to the molecular weight the end groups of the RAFT CTA were not visible by ^{1}H NMR spectroscopy therefore homopolymer **1** was determined to have a degree of polymerization (DP) of 400 by conversion NMR. For homopolymer **2** a DP of 125 was determined by comparison of end group signals between δ 7.50–8.10 ppm relative to the polymer peaks at 3.0 ppm and 3.34 ppm (see ESI). This matched well with that predicted from conversion. The absolute M_w of polymer **1** was determined by static light scattering (SLS) in 0.5 M NaCl solution to be 136 kDa, which is in good agreement with the M_n, 111.6 kDa calculated from ^{1}H NMR (see ESI).

*3.2. Synthesis of PDMAPS-b-PMMA diblocks, **3** and **4***

*3.2.1. Synthesis of **3** via polymerization in HFIP*

As previously discussed, the ability to synthesize sulfobetaine-hydrophobic block copolymers is interesting due to their potential self-assembly and thermo-responsive behavior. However, the direct synthesis of such block copolymers has not yet been reported as polybetaines have poor solubility, often only being soluble in water, either at high temperatures or in the presence of salt [4], or highly fluorinated polar solvents such as HFIP [5]. Such highly fluorinated solvents are not widely used in polymer synthesis due, in part, to their associated hazards. This has limited the synthesis, and subsequent solution-based characterization, of betaine-containing amphiphilic block copolymers. Since HFIP is a good solvent for both PDMAPS and MMA, chain extension of **1** was carried out in this solvent (see Scheme 1). The polymer was purified by dialysis against water and recovered by lyophilization to yield **3**, M_n (^{1}H NMR) = 121.7 kDa, M_n (HFIP SEC) = 73.1, $Đ_M$ = 1.34. The efficient chain



Scheme 1. Synthetic routes to the diblock copolymers **3** and **4**.

extension can be seen in the shift in the molecular weight of the HFIP SEC chromatogram of the starting sulfobetaine homopolymer and the resulting diblock copolymer (see Fig. 1). The narrow dispersity obtained and the retention of the RAFT end group, observed from the SEC UV trace recorded at 309 nm (see ESI), indicates a good degree of control over the polymerization.

The length of the MMA block was calculated to be 100 by ^{1}H NMR spectroscopy by comparison of the starting homopolymer, **1**, and the diblock copolymer, **3** in deuterated HFIP (see ESI).

3.3. Emulsion polymerization

Oil-in-water emulsion polymerization is a common method used to synthesize amphiphilic block copolymers in water where the starting homopolymer and the growing second block have differing solubility.[50–52] Therefore in order to compare the HFIP chain extension reaction to a completely aqueous system, homopolymer **2** was chain extended with MMA in 0.5 M NaCl solution as an oil-in-water emulsion polymerization. During reaction the solution became opalescent, which is indicative of particles having formed as expected in an emulsion polymerization. The resulting polymer was purified by dialysis, recovered by lyophilization then precipitated from HFIP into hexanes and dried to yield **4**, M_n (^{1}H NMR) = 52.2 kDa, M_n (HFIP SEC) = 31.6 kDa, $Đ_M$ = 1.80. The length of the hydrophobic block was determined to be 181 units from ^{1}H NMR spectroscopy in deuterated HFIP (see Fig. 2). The dispersity observed in the HFIP SEC is high and significant tailing can be seen, indicating a lack of control and inefficient chain extension (see ESI). The significantly lower degree of tailing observed in the SEC chromatogram of **3** compared to that of **4**, along with the much lower dispersity obtained, indicates that HFIP is a better solvent for the chain extension of PDMAPS with MMA than 0.5 M NaCl.

3.4. Self-assembly of PDMAPS-b-PMMA diblocks

Previous reports by our group showed that the addition of hydrophilic POEGMA to PDMAPS polymers resulted in the overall hydrophilicity of the DMAPS increasing and therefore lowering the temperature at which the block becomes hydrophilic [22,29]. Conversely, incorporation of hydrophobic comonomers into UCST polymers has resulted in an increase in the UCST cloud point temperatures [36]. Agarwal and co-workers have shown that the copolymerization of hydrophobic acrylonitrile with acrylamide causes the polymer to display a UCST and increasing the amounts of acrylonitrile raises the UCST [53]. Similar effects are seen with styrene as the hydrophobic comonomer [54]. However, the effect of adding a hydrophobic block to a UCST polymer is unknown. Therefore it may be expected that chain extending the DMAPS homopolymer with the hydrophobic MMA may cause an increase in the UCST cloud point.

Diblock copolymer **3** was self-assembled by direct dissolution into water at 25 °C at a concentration of 1 mg mL^{-1}. The size of the structures at 25 °C was 67 ± 3 nm as observed by DLS analysis and TEM analysis confirms the presence of micelles with an average size of 50 ± 12 nm (see Fig. 3).

The temperature response of **3** was investigated by DLS between 5 °C and 65 °C and size measured every 10 °C. Based on the UCST cloud point of the homopolymer **1** (19 °C) it would be expected that below this temperature the PDMAPS block would become completely hydrophobic and therefore precipitation would occur, however this was not observed. Indeed, even at 5 °C the micelles had shrunk to 59 ± 2 nm but remained stable in solution. Conversely, heating to 65 °C caused swelling of structures to 81 ± 2 nm (see Fig. 4).

Diblock copolymer **4** was also self-assembled in water by direct dissolution at 1 mg mL^{-1}. Analysis by DLS gives a population with D_h = 98 ± 8 nm whilst TEM analysis showed the presence of spherical structures with an average size of 60 ± 10 nm (see Fig. 5). The smaller size observed by TEM analysis is a result of drying effects during the TEM sample preparation [55].

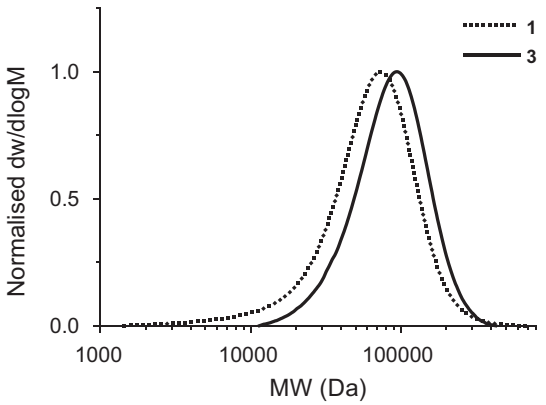


Fig. 1. HFIP SEC chromatograms showing the shift in molecular weight upon chain extension from homopolymer **1** to diblock copolymer **3**.

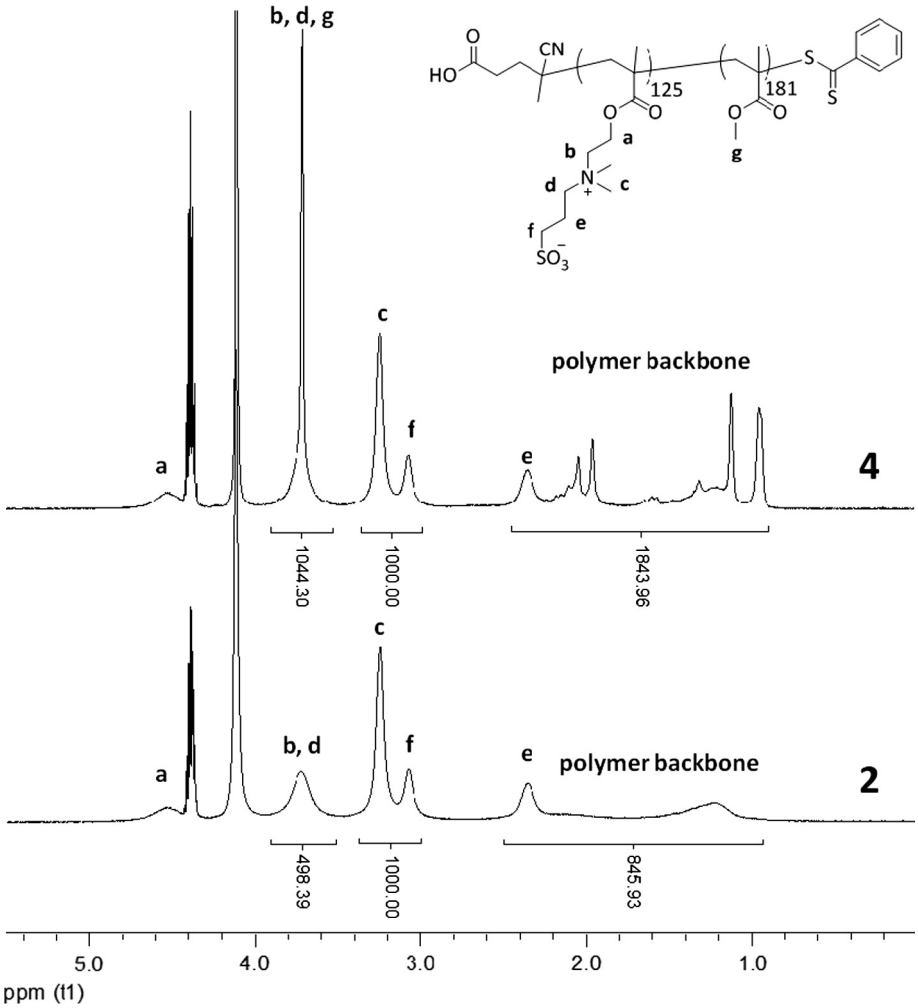


Fig. 2. ^{1}H NMR spectra of homopolymer **2** and diblock copolymer **4** in deuterated HFIP, showing the appearance of the MMA peaks at 3.6 ppm and 0.9–1.2 ppm, recorded at 45 °C and 500 MHz.

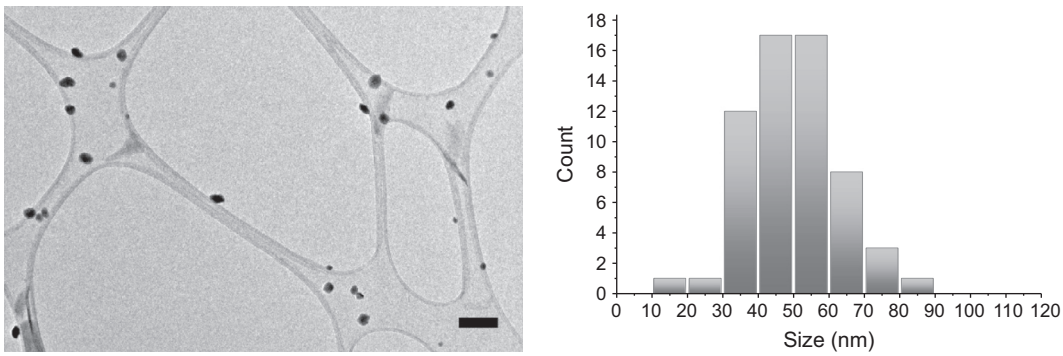


Fig. 3. TEM of **3** at 0.1 mg mL^{-1} on graphene oxide, scale bar = 200 nm and the distribution of sizes observed.

Variable temperature DLS was conducted on a 1 mg mL^{-1} solution of **4** in 18.2 MΩ cm^{-1} water from 5 °C to 65 °C with the size being measured every 5 °C. Although the homopolymer **2** displays no UCST due to its low molecular weight, the proximity of the chains in a self-assembled structure will increase the local concentration and therefore could force a thermoresponse. However, there was no significant size change across the temperature range investigated (see ESI).

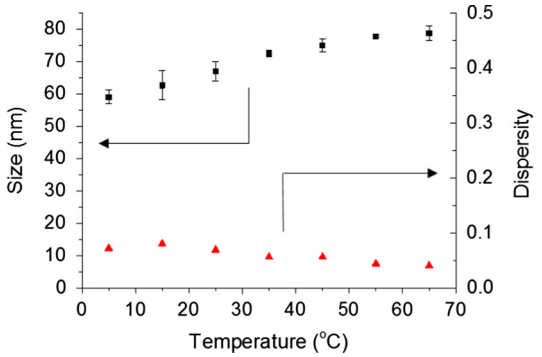


Fig. 4. Plot of D_h *vs* temperature and dispersity *vs* temperature for a 1 mg mL^{-1} solution of diblock copolymer **3** in water.

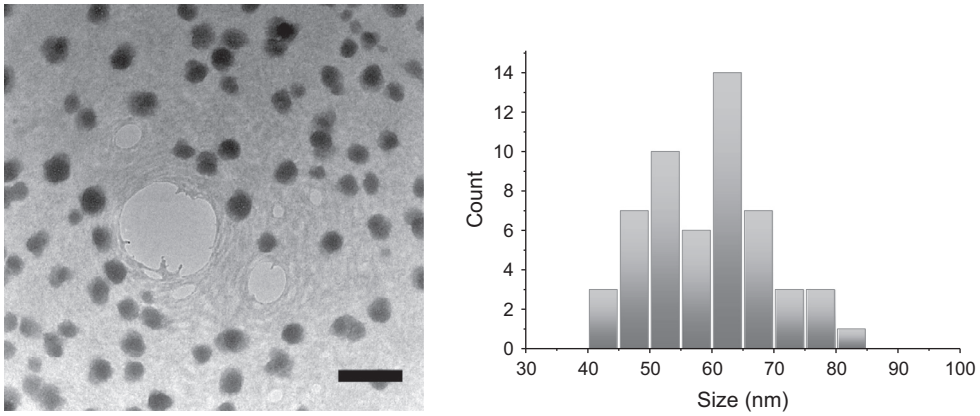


Fig. 5. TEM image of micelles of **4** at 0.1 mg mL^{-1} on graphene oxide, scale bar = 200 nm, and the distribution of sizes observed.

3.5. Investigation of the micelle swelling behavior by ^{1}H NMR spectroscopy

In order to further investigate the thermo-responsive behavior of diblock copolymer **3**, variable temperature ^{1}H NMR was conducted. A solution of **3** was made at 5 mg mL^{-1} in D_2O. ^{1}H NMR spectroscopy was performed at temperatures ranging from 5 to 65 °C every 10 °C. A small amount of DMF was used as an internal standard to help calculate the percentage hydrophilicity of the polymer. The COH peak of the DMF was set at an integration of 1 and three separate peaks relating to the DMAPS block were integrated relative to this DMF peak (see Fig. 6). The integration of each peak at the highest temperature was assumed to be fully hydrated, *i.e.* all the available DMAPS side chains are hydrated and therefore hydrophilic. The integrations of the same peaks at different temperatures were compared to these fully hydrated peaks to calculate the percentage hydrophilicity present in the polymer at that temperature.

Fig. 6 shows how the integrations of the DMAPS peaks change with temperature. The betaine block never becomes fully hydrophobic, even at temperatures of 5 °C approximately 35% of the block remains hydrated. The PMMA block is not visible as it is not solvated [30]. This remaining hydrophilicity prevents the polymers from macroscopically aggregating, even at temperatures well below the UCST cloud point of the PDMAPS block. This retained hydrophilicity is similar to that observed by our group when studying a diblock copolymer consisting of a short block of POEGMA and a much longer PDMAPS block. Here, the PDMAPS block also retained significant levels of hydrophilicity at temperatures well below the UCST cloud point [29]. In another similar example by Willcock et al. the UCST cloud points of linear and branched homopolymers of PDMAPS were studied. The branched homopolymers displayed greatly reduced cloud points, compared to the linear homopolymers [22]. It was proposed that the shorter chains of PDMAPS in the branched polymers acted as stabilizers, forming a core-shell structure and therefore remaining in solution. Our results, along with these previous studies, show that the thermo-responsive behavior of DMAPS within a higher order polymer structure is complicated and the temperature at which the polymer exhibits a response is affected, regardless of whether the other block is hydrophilic or hydrophobic [56].

3.6. Investigation of the swelling behavior of **3** by SLS

In order to prove that the size change was a result of the swelling of the PDMAPS block, rather than a further aggregation of the assembled structures, SLS and multi-angle DLS at 20 °C and 60 °C was performed at concentrations between 0.5 and

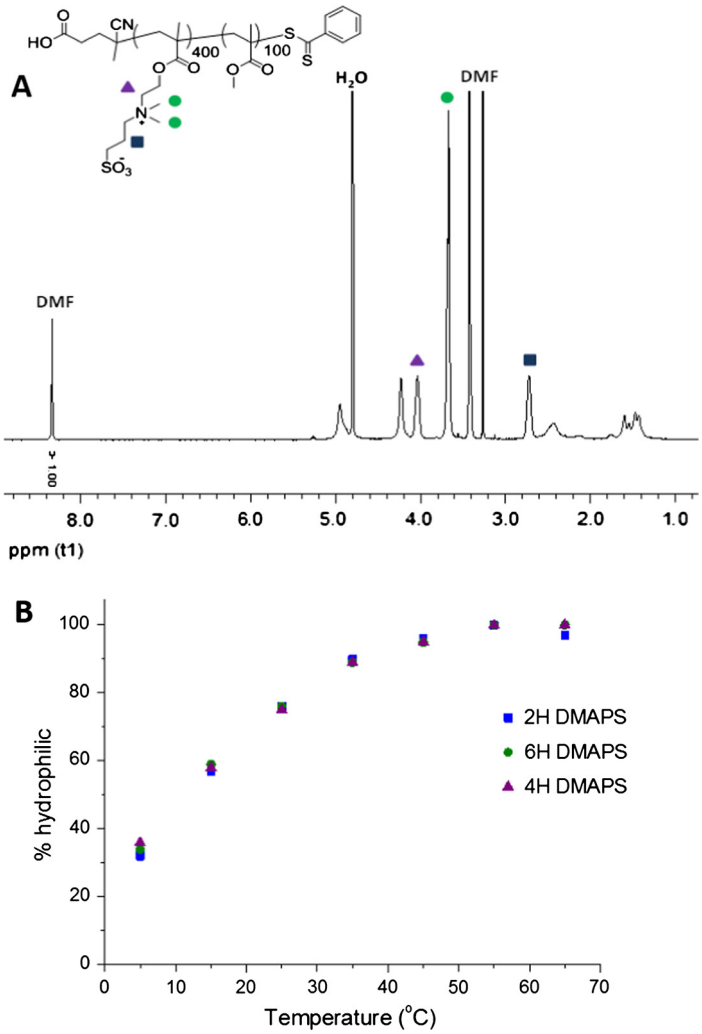


Fig. 6. (Top) ^{1}H NMR spectrum of diblock copolymer **3** in D_2O, showing the three DMAPS peaks used for calculating remaining hydrophilicity, recorded at 65 °C and 500 MHz. (Bottom) Graph showing how the % hydrophilicity of the PDMAPS block of diblock **3** changes with temperature.

2 mg mL^{-1}. Plotting the apparent diffusion coefficient for each concentration against concentration yields the translational diffusion coefficient, yielding a D_h = 72 nm at 20 °C and 87 nm at 60 °C (see Fig. 7).

$Kc/R_{\theta,fast}$ was plotted against q^2 for each concentration and each plot extrapolated to zero angle. The extrapolated $Kc/R_{\theta,fast}$ value was then plotted against concentration and extrapolated to zero concentration, which was used to determine the absolute molecular weight of the nanostructure at each temperature. The absolute molecular weight of the self-assembled structures of **3** was determined to be 27.5 MDa at 20 °C and 27.6 MDa at 60 °C (see Fig. 7). The R_g/R_h ratio at 20 °C was calculated to be 0.78 and at 60 °C was 0.71.

The similar molecular weights of the micelles at 20 °C and 60 °C indicates that there has been no change in the aggregation number of the structures at the different temperatures. The difference in size is evident from the hydrodynamic diameters calculated (73 nm at 20 °C and 86 nm at 60 °C) and therefore this increase in size but not molecular weight confirms that the swelling seen is solely due to the hydration of the DMAPS block, as expected, and not any difference in aggregation of the polymer chains.

3.7. Release of hydrophobic payloads from the swollen micelle

At low temperatures the micelles formed by **3** are collapsed as the PDMAPS block is mainly hydrophobic. This means that the hydrophobic core will be larger due to the permanently hydrophobic PMMA block and the hydrophobic portion of the PDMAPS. At higher temperatures the PDMAPS block becomes hydrophilic and hydrated and so the hydrophobic core of the

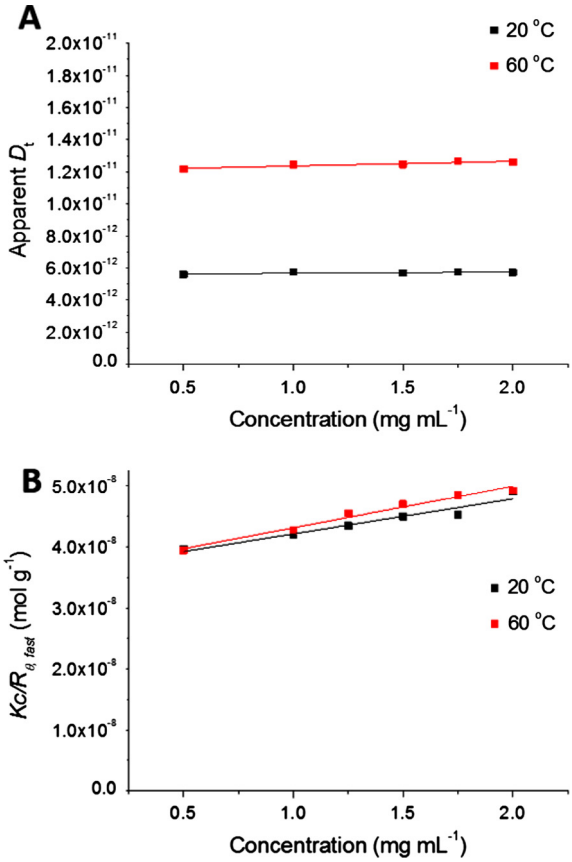


Fig. 7. (Top) Plot of apparent D_t against concentration for diblock **3** at 20 °C and 60 °C. The intercepts of the linear fits correspond to the hydrodynamic diameters. (Bottom) Plot of $Kc/R_{\theta,fast}$ *vs* concentration for self-assembled solutions of **3** at 20 °C and 60 °C. The M_w of the micelles was calculated using the intercept of the linear fit to the SLS data.

micelles is smaller at elevated temperatures. Therefore it should be possible to encapsulate a hydrophobic payload within the core of the micelles at low temperatures and then release some of the payload at higher temperatures.

A 1 mg mL^{-1} solution of **3** was stirred overnight at 4 °C with Nile Red at 1 mg mL^{-1}. The solution was then filtered through a 0.45 μm nylon filter in order to remove any non-encapsulated Nile Red and the sample tested for fluorescence (λ_{ex} = 550 nm, λ_{em} = 575 nm). There was a significant fluorescence response. The solution was then heated at 65 °C for 10 min, and then filtered whilst hot. The fluorescence response had significantly decreased, showing that Nile Red had been released from the micelles upon heating (see Fig. 8). This demonstrates that even though the micelle remains intact throughout the temperature range, a significant proportion of Nile Red is released as the size of the hydrophobic core decreases. The effect of filtering the micellar solution upon fluorescence intensity was investigated and it was shown that the small

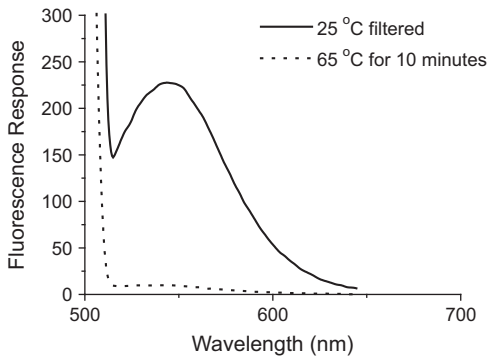


Fig. 8. Plot of fluorescence of micelles of **3** loaded with Nile Red before and after heating at 65 °C for 10 min.

decrease in intensity as a result of loss of micelles on the filter was not significant (see ESI) and therefore the significant decrease in the fluorescence signal is a result of the release of the Nile Red from the core of the micelles.

4. Conclusions

The direct synthesis of well-defined amphiphilic polybetaine block copolymers by RAFT polymerization in HFIP has been achieved and demonstrated to offer greater control than the corresponding RAFT emulsion polymerization of MMA. The incorporation of the permanently hydrophobic PMMA block was shown to direct the assembly of the polymers into micelles, and whilst the PDMAPS homopolymer displays a UCST cloud point, the resultant micelle instead demonstrated a swelling behavior in response to increased temperature. SLS conducted at 20 °C and 60 °C prove that the swelling is a result of the solvation of the PDMAPS block and not a change in aggregation state. Variable temperature ^{1}H NMR showed that the PDMAPS block never becomes fully hydrophobic, explaining the presence of stable micelles at temperatures well below the UCST of the betaine homopolymer. This swelling behavior has been exploited to release a hydrophobic payload from the core of the micelle. This work confirms that the architecture of stimuli-responsive materials has a huge effect on their responsive behavior, demonstrating the need for structure control when incorporating them into higher order structures.

Acknowledgements

The authors would like to thank the EPSRC, the University of Warwick and the ERC for funding.

Appendix A. Supplementary material

Supplementary data associated with this article can be found, in the online version, at http://dx.doi.org/10.1016/j.eurpolymj.2016.09.002.

References

[1] A.B. Lowe, C.L. McCormick, Synthesis and solution properties of zwitterionic polymers, Chem. Rev. 102 (11) (2002) 4177–4190.
[2] J. Seuring, S. Agarwal, Polymers with upper critical solution temperature in aqueous solution, Macromol. Rapid Commun. 33 (22) (2012) 1898–1920.
[3] B. Yu, A.B. Lowe, K. Ishihara, RAFT synthesis and stimulus-induced self-assembly in water of copolymers based on the biocompatible monomer 2-(methacryloyloxy)ethyl phosphorylcholine, Biomacromolecules 10 (4) (2009) 950–958.
[4] J.C. Salamone, W. Volksen, A.P. Olson, S.C. Israel, Aqueous solution properties of a poly(vinyl imidazolium sulphobetaine), Polymer 19 (10) (1978) 1157–1162.
[5] V.M. Monroy Soto, J.C. Galin, Poly(sulphopropylbetaines): 1. Synthesis and characterization, Polymer 25 (1) (1984) 121–128.
[6] R. Hart, D. Timmerman, New polyampholytes: the polysulfobetaines, J. Polym. Sci. 28 (118) (1958) 638–640.
[7] S. Nakai, T. Nakaya, M. Imoto, Polymeric phospholipid analog. 10. Synthesis and polymerization of 2-(methacryloyloxy)ethyl 2-aminoethyl hydrogen phosphate, Makromol. Chem. 178 (10) (1977) 2963–2967.
[8] H. Ladenheim, H. Morawetz, A new type of polyampholyte: poly(4-vinyl pyridine betaine), J. Polym. Sci. 26 (113) (1957) 251–254.
[9] Y.J. Shih, Y. Chang, A. Deratani, D. Quemener, "Schizophrenic" hemocompatible copolymers via switchable thermoresponsive transition of nonionic/zwitterionic block self-assembly in human blood, Biomacromolecules 13 (9) (2012) 2849–2858.
[10] S.L. West, J.P. Salvage, E.J. Lobb, S.P. Armes, N.C. Billingham, A.L. Lewis, G.W. Hanlon, A.W. Lloyd, The biocompatibility of crosslinkable copolymer coatings containing sulfobetaines and phosphobetaines, Biomaterials 25 (7–8) (2004) 1195–1204.
[11] Y. Chang, S.C. Liao, A. Higuchi, R.C. Ruaan, C.W. Chu, W.Y. Chen, A highly stable nonbiofouling surface with well-packed grafted zwitterionic polysulfobetaine for plasma protein repulsion, Langmuir 24 (10) (2008) 5453–5458.
[12] Y. Chang, S.H. Shu, Y.J. Shih, C.W. Chu, R.C. Ruaan, W.Y. Chen, Hemocompatible mixed-charge copolymer brushes of pseudozwitterionic surfaces resistant to nonspecific plasma protein fouling, Langmuir 26 (5) (2009) 3522–3530.
[13] Y.J. Shih, Y. Chang, Tunable blood compatibility of polysulfobetaine from controllable molecular-weight dependence of zwitterionic nonfouling nature in aqueous solution, Langmuir 26 (22) (2010) 17286–17294.
[14] J. Yuan, X. Huang, P. Li, L. Li, J. Shen, Surface-initiated RAFT polymerization of sulfobetaine from cellulose membranes to improve hemocompatibility and antibiofouling property, Polym. Chem. 4 (19) (2013) 5074–5085.
[15] K. Seetho, S. Zhang, K.A. Pollack, J. Zou, J.E. Raymond, E. Martinez, K.L. Wooley, Facile synthesis of a phosphorylcholine-based zwitterionic amphiphilic copolymer for anti-biofouling coatings, ACS Macro Lett. 4 (5) (2015) 505–510.
[16] F. Dai, Y. Liu, W. Wang, W. Liu, Stable gene transfection mediated by polysulfobetaine/PDMAEMA diblock copolymer in salted medium, J. Biomater. Sci. Polym. Ed. 24 (3) (2013) 330–343.
[17] Y. Chang, Y.-J. Shih, C.-J. Lai, H.-H. Kung, S. Jiang, Blood-inert surfaces via ion-pair anchoring of zwitterionic copolymer brushes in human whole blood, Adv. Funct. Mater. 23 (9) (2013) 1100–1110.
[18] K.-T. Huang, Y.-L. Fang, P.-S. Hsieh, C.-C. Li, N.-T. Dai, C.-J. Huang, Zwitterionic nanocomposite hydrogels as effective wound dressings, J. Mater. Chem. B 10 (2016) 10.
[19] D.N. Schulz, D.G. Peiffer, P.K. Agarwal, J. Larabee, J.J. Kaladas, L. Soni, B. Handwerker, R.T. Garner, Phase behavior and solution properties of sulphobetaine polymers, Polymer 27 (11) (1986) 1734–1742.
[20] M. Noh, Y. Mok, D. Nakayama, S. Jang, S. Lee, T. Kim, Y. Lee, Introduction of pH-sensitive upper critical solution temperature (UCST) properties into branched polyethylenimine, Polymer 54 (20) (2013) 5338–5344.
[21] M. Arotçaréna, B. Heise, S. Ishaya, A. Laschewsky, Switching the inside and the outside of aggregates of water-soluble block copolymers with double thermoresponsivity, J. Am. Chem. Soc. 124 (14) (2002) 3787–3793.
[22] H. Willcock, A. Lu, C.F. Hansell, E. Chapman, I.R. Collins, R.K. O'Reilly, One-pot synthesis of responsive sulfobetaine nanoparticles by RAFT polymerisation: the effect of branching on the UCST cloud point, Polym. Chem. 5 (2014) 1023–1030.
[23] M.S. Donovan, A.B. Lowe, T.A. Sanford, C.L. McCormick, Sulfobetaine-containing diblock and triblock copolymers via reversible addition-fragmentation chain transfer polymerization in aqueous media, J. Polym. Sci., Part A: Polym. Chem. 41 (9) (2003) 1262–1281.
[24] D. Wang, T. Wu, X. Wan, X. Wang, S. Liu, Purely salt-responsive micelle formation and inversion based on a novel schizophrenic sulfobetaine block copolymer: structure and kinetics of micellization, Langmuir 23 (23) (2007) 11866–11874.

[25] Z. Tuzar, H. Pospisil, J. Plestil, A.B. Lowe, F.L. Baines, N.C. Billingham, S.P. Armes, Micelles of hydrophilic–hydrophobic poly(sulfobetaine)-based block copolymers, Macromolecules 30 (8) (1997) 2509–2512.
[26] A.B. Lowe, N.C. Billingham, S.P. Armes, Synthesis and properties of low-polydispersity poly(sulfopropylbetaine)s and their block copolymers, Macromolecules 32 (7) (1999) 2141–2148.
[27] Y. Zhu, J.-M. Noy, A.B. Lowe, P.J. Roth, The synthesis and aqueous solution properties of sulfobutylbetaine (co)polymers: comparison of synthetic routes and tuneable upper critical solution temperatures, Polym. Chem. 6 (31) (2015) 5705–5718.
[28] M. Tasso, E. Giovanelli, D. Zala, S. Bouccara, A. Fragola, M. Hanafi, Z. Lenkei, T. Pons, N. Lequeux, Sulfobetaine-vinylimidazole block copolymers: a robust quantum dot surface chemistry expanding bioimaging's horizons, ACS Nano 9 (11) (2015) 11479–11489.
[29] K.E.B. Doncom, A. Pitto-Barry, H. Willcock, A. Lu, B.E. McKenzie, N. Kirby, R.K. O'Reilly, Complementary light scattering and synchrotron small-angle X-ray scattering studies of the micelle-to-unimer transition of polysulfobetaines, Soft Matter 11 (18) (2015) 3666–3676.
[30] V. Butun, C.E. Bennett, M. Vamvakaki, A.B. Lowe, N.C. Billingham, S.P. Armes, Selective betainisation of tertiary amine methacrylate block copolymers, J. Mater. Chem. 7 (9) (1997) 1693–1695.
[31] A.B. Lowe, N.C. Billingham, S.P. Armes, Synthesis of polybetaines with narrow molecular mass distribution and controlled architecture, Chem. Commun. 13 (1996) 1555–1556.
[32] M. Vamvakaki, N.C. Billingham, S.P. Armes, Synthesis of novel block and statistical methacrylate-based ionomers containing acidic, basic or betaine residues, Polymer 39 (11) (1998) 2331–2337.
[33] I.V. Berlinova, I.V. Dimitrov, R.G. Kalinova, N.G. Vladimirov, Synthesis and aqueous solution behavior of copolymers containing sulfobetaine moieties in side chains, Polymer 41 (3) (2000) 831–837.
[34] Q. Sun, Y. Su, X. Ma, Y. Wang, Z. Jiang, Improved antifouling property of zwitterionic ultrafiltration membrane composed of acrylonitrile and sulfobetaine copolymer, J. Membr. Sci. 285 (1–2) (2006) 299–305.
[35] M. Cai, M. Leng, A. Lu, L. He, X. Xie, L. Huang, Y. Ma, J. Cao, Y. Chen, X. Luo, Synthesis of amphiphilic copolymers containing zwitterionic sulfobetaine as pH and redox responsive drug carriers, Colloids Surf., B 126 (2015) 1–9.
[36] P.A. Woodfield, Y. Zhu, Y. Pei, P.J. Roth, Hydrophobically modified sulfobetaine copolymers with tunable aqueous UCST through postpolymerization modification of poly(pentafluorophenyl acrylate), Macromolecules 47 (2) (2014) 750–762.
[37] R.H. Brown, A.J. Duncan, J.-H. Choi, J.K. Park, T. Wu, D.J. Leo, K.I. Winey, R.B. Moore, T.E. Long, Effect of ionic liquid on mechanical properties and morphology of zwitterionic copolymer membranes, Macromolecules 43 (2) (2010) 790–796.
[38] R.H. Brown, M.T. Hunley, J.M.H. Allen, T.E. Long, Electrospinning zwitterion-containing nanoscale acrylic fibers, Polymer 50 (20) (2009) 4781–4787.
[39] M. Ehrmann, J.-C. Galin, Statistical n-butyl acrylate-sulphonatopropylbetaine copolymers: 1. Synthesis and molecular characterization, Polymer 33 (4) (1992) 859–865.
[40] M. Gauthier, T. Carrozzella, A. Penlidis, Sulfobetaine zwitterionomers based on n-butyl acrylate and 2-ethoxyethyl acrylate: monomer synthesis and copolymerization behavior, J. Polym. Sci., Part A: Polym. Chem. 40 (4) (2002) 511–523.
[41] Veronika Strehmel, A. Laschewsky, Hendrik Wetzel, Homopolymerization of a highly polar zwitterionic methacrylate in ionic liquids and its copolymerization with a non-polar methacrylate, e-Polymers 6 (1) (2006) 131–140.
[42] E. Kamenska, B. Kostova, I. Ivanov, D. Rachev, G. Georgiev, Emulsifier-free emulsion copolymerization of vinyl acetate and 3-dimethyl (methacryloyloxyethyl)ammonium propanesulfonate and swelling behavior of their copolymer matrices, Macromol. React. Eng. 1 (5) (2007) 553–562.
[43] B. Kostova, E. Kamenska, D. Rachev, S. Simeonova, G. Georgiev, K. Balashev, Polyzwitterionic copolymer nanoparticles loaded in situ with metoprolol tartrate: synthesis, morphology and drug release properties, J. Polym. Res. 20 (2) (2013) 1–8.
[44] Y.-L. Zheng, M. Galin, J.-C. Galin, Random ethylacrylate-sulphonatopropylbetaine copolymers. 1. Synthesis and characterization, Polymer 29 (4) (1988) 724–730.
[45] V. Strehmel, H. Wetzel, A. Laschewsky, E. Moldenhauer, T. Klein, Influence of imidazolium-based ionic liquids on the synthesis of amphiphilic copolymers based on n-butylmethacrylate and a zwitterionic methacrylate, Polym. Adv. Technol. 19 (10) (2008) 1383–1390.
[46] J. Jakes, Regularized positive exponential sum (REPES) program – a way of inverting laplace transform data obtained by dynamic light scattering, Collect. Czech. Chem. Commun. 60 (1995) 1781–1797.
[47] J.P. Patterson, A.M. Sanchez, N. Petzetakis, T.P. Smart, I.I.I.T.H. Epps, I. Portman, N.R. Wilson, R.K. O'Reilly, A simple approach to characterizing block copolymer assemblies: graphene oxide supports for high contrast multi-technique imaging, Soft Matter 8 (12) (2012) 3322–3328.
[48] N.R. Wilson, P.A. Pandey, R. Beanland, R.J. Young, I.A. Kinloch, L. Gong, Z. Liu, K. Suenaga, J.P. Rourke, S.J. York, J. Sloan, Graphene oxide: structural analysis and application as a highly transparent support for electron microscopy, ACS Nano 3 (9) (2009) 2547–2556.
[49] N. Petzetakis, M.P. Robin, J.P. Patterson, E.G. Kelley, P. Cotanda, P.H.H. Bomans, N.A.J.M. Sommerdijk, A.P. Dove, T.H. Epps, R.K. O'Reilly, Hollow block copolymer nanoparticles through a spontaneous one-step structural reorganization, ACS Nano 7 (2) (2013) 1120–1128.
[50] S. Boisse, J. Rieger, K. Belal, A. Di-Cicco, P. Beaunier, M.-H. Li, B. Charleux, Amphiphilic block copolymer nano-fibers via RAFT-mediated polymerization in aqueous dispersed system, Chem. Commun. 46 (11) (2010) 1950–1952.
[51] E. Groison, S. Brusseau, F. D'Agosto, S. Magnet, R. Inoubli, L. Couvreur, B. Charleux, Well-defined amphiphilic block copolymer nanoobjects via nitroxide-mediated emulsion polymerization, ACS Macro Lett. 1 (1) (2012) 47–51.
[52] X. Zhang, S. Boissé, W. Zhang, P. Beaunier, F. D'Agosto, J. Rieger, B. Charleux, Well-defined amphiphilic block copolymers and nano-objects formed in situ via RAFT-mediated aqueous emulsion polymerization, Macromolecules 44 (11) (2011) 4149–4158.
[53] J. Seuring, S. Agarwal, First example of a universal and cost-effective approach: polymers with tunable upper critical solution temperature in water and electrolyte solution, Macromolecules 45 (9) (2012) 3910–3918.
[54] B.A. Pineda-Contreras, F. Liu, S. Agarwal, Importance of compositional homogeneity of macromolecular chains for UCST-type transitions in water: controlled versus conventional radical polymerization, J. Polym. Sci., Part A: Polym. Chem. 52 (13) (2014) 1878–1884.
[55] J.P. Patterson, M.P. Robin, C. Chassenieux, O. Colombani, R.K. O'Reilly, The analysis of solution self-assembled polymeric nanomaterials, Chem. Soc. Rev. (2014).
[56] M.I. Gibson, R.K. O'Reilly, To aggregate, or not to aggregate? considerations in the design and application of polymeric thermally-responsive nanoparticles, Chem. Soc. Rev. 42 (17) (2013) 7204–7213.